Applied Catalysis B: Environmental 343 (2024) 123538

Contents lists available at ScienceDirect

Applied Catalysis B: Environmental

journal homepage: www.elsevier.com/locate/apcatb

Adsorption behavior of atmospheric CO_2 with/without water vapor on CeO_2 surface

Masato Akatsuka [a], Akira Nakayama [b], Masazumi Tamura [a,*]

[a] Department of Chemistry and Bioengineering, School of Engineering, Osaka Metropolitan University, 3-3-138, Sugimoto, Sumiyoshi-ku, Osaka 558-8585, Japan
[b] Department of Chemical System Engineering, Graduate School of Engineering, The University of Tokyo, 7-3-1, Hongo, Bunkyo-ku, Tokyo 113-8656, Japan

ARTICLE INFO

Keywords:
CeO_2
Carbon dioxide
FT-IR
Water vapor
Atmospheric CO_2
DFT calculations

ABSTRACT

The significance of investigations into CO_2 adsorption from the air has been steadily on the rise in recent years. CeO_2 is known as an effective catalyst for CO_2 transformation and adsorbent of CO_2, however, the study on the adsorption of low concentrations of CO_2 on CeO_2 and the effect of water vapor on the adsorption of CO_2 on CeO_2 is very limited. Herein, the adsorption behavior of low concentration of CO_2, particularly atmospheric CO_2 (0.04 vol%), on CeO_2 and the effect of water vapor on the CO_2 adsorption were investigated by *in situ* FT-IR, mass spectroscopies, and DFT calculations. Low concentrations of CO_2 can be effectively adsorbed on CeO_2, and typical four CO_2 adspecies such as bidentate carbonate, hydrogen carbonate, monodentate carbonate, and polydentate carbonate were formed on CeO_2. The CO_2 adsorption amount on CeO_2 was increased by 20% by the presence of water vapor compared with that in the absence of water vapor. Based on FT-IR analyses and DFT calculations, the adsorption strength of CO_2 is comparable to that of water on CeO_2, and the water adspecies will assist the adsorption of CO_2 via hydrogen bonding, leading to the increase of CO_2 adsorption amount.

1. Introduction

Global warming is an urgent issue all over the world, which causes various problems such as dangerous weather events, drought, rising sea levels, melting glaciers, and so on, and these problems will become a threat to human life and communities [1,2]. CO_2 is a main gas of greenhouse effect gases, and hence the development of new methods for decreasing the CO_2 concentration in the air is highly required. Various CO_2 adsorption methods such as physical and chemical adsorption methods using amine-based adsorbents and porous materials and so on have been intensively developed and commercialized [3,4]. Direct air capture (DAC) is also a highly promising solution for extracting carbon dioxide directly from the atmosphere because the technology is independent of the origin of CO_2 emissions and enables strategic placement of capture facilities in areas with optimal energy economics or robust access to renewable energy [4–6]. The development of CO_2 transformation methods is also of great importance as well as the CO_2 capture technologies. One of the promising methods is the chemical transformation of CO_2 into valuable chemicals [7–11] because the chemical transformation can fix CO_2 into chemicals and contribute to carbon recycling. The combination of these methods is called carbon dioxide capture and utilization (CCU), where CO_2 capture including CO_2 adsorption and desorption, and CO_2 transformation to valuable chemicals are typically consecutive processes. However, the separation and purification in the CO_2 capture process are usually energy-consuming because the desorption of the captured CO_2 generally requires heating, namely large energy [11]. Recently, integrated capture and conversion of CO_2 by using materials with both functions of CO_2 adsorption ability and catalysis have attracted attention, and various homogeneous and heterogeneous catalyst systems have been developed. Main researches with homogeneous catalysts are as follows: The combination of CO_2 capture and hydrogenation to methanol using complex catalysts, mainly Ru complexes, and the combination of CO_2 capture and hydrogenation to formic acid derivatives using Rh, Ru, Ir complexes, and so on [12]. Considering the reusability and stability of catalysts, heterogeneous catalysts are preferable to homogeneous ones. As for heterogeneous catalysts, basic metal oxides have been reported to be effective for the capture of CO_2 due to the base property, and the combination of metal species such as Ni, Ru, Rh, Pt, and Cu with the basic metal oxides such as CaO, MgO and Na_2CO_3 are used for the CO_2 capture and conversions such as hydrogenation to methane, reverse water-gas shift reaction, reforming with alkanes and hydrogenation to methanol [13–19].

* Corresponding author.
E-mail address: mtamura@omu.ac.jp (M. Tamura).

https://doi.org/10.1016/j.apcatb.2023.123538
Received 13 September 2023; Received in revised form 14 November 2023; Accepted 19 November 2023
Available online 22 November 2023

However, the report on only metal oxides having both functions of the CO_2 capture and conversion is very limited, and to our best knowledge, $Fe_5Co_5Mg_{10}CaO$ is only the metal oxide, which is effective for CO_2 capture and reverse water-gas shift reaction at 923 K to show 90% conversion of CO_2 and high selectivity (>99%) to CO [20]. Therefore, the development of effective solid catalyst systems having both functions of CO_2 capture and transformation is highly required.

Cerium oxide (CeO_2) has unique acid/base and redox properties and is often used as catalysts or catalyst supports for various gas-phase and liquid-phase reactions [21–30]. It is well-known that CeO_2 is an effective heterogeneous catalyst for the conversion of CO_2 with alcohols and/or amines, and the corresponding carbonate derivatives such as organic (poly)carbonates [31–48], carbamates [49–61] and ureas [52,53] are produced in high yields with high-pressure and/or high-concentration CO_2. Recently, Tomishige and co-workers reported that CeO_2 catalyzed the conversion of ethylenediamine carbamate prepared from CO_2 and ethylenediamine to ethylene urea in high yields in the absence of external CO_2 [54–56]. These results indicate that CeO_2 can catalyze the carboxylation of amines under a low CO_2 pressure or a low concentration of CO_2, which presents the possibility of CO_2 transformations under a low concentration of CO_2 or without additional CO_2 over a CeO_2 catalyst. In the transformation of CO_2 to carbonate derivatives over CeO_2-based catalysts, the acid-base bifunctionality of CeO_2 was generally reported to be responsible for the activation of CO_2 and methanol and/or amines [21,26,28,29,57,58], and based on the correlation between the basic site amount and CO_2 formation rate (or amount) in the synthesis of organic carbonates, the acid-base site was proposed to be the main active site of CeO_2-based catalysts [44,59–62]. On the other hand, the oxygen vacancy site of CeO_2 was reported to be the active site of CO_2 mainly in the reductive transformation of CO_2, such as CO_2 methanation, CO_2 hydrogenation, water-gas shift reaction, dry reforming, and so on [63,64], which will be related to the redox property of CeO_2. Recently, the oxygen vacancy site was reported to be effective for the activation of CO_2 also in the organic carbonate syntheses based on XANES analyses [65]. DFT calculation on CO_2 adsorption on CeO_2 (111), which is the most stable facet, reported that CO_2 can be adsorbed and activated by the basic site or acid-based site as monodentate and bidentate CO_2 adspecies, which are the main adspecies of CO_2 on CeO_2, leading to the bending of the C-O-C bond and the elongation of the C-O bond [66]. The activation mode was supported by FT-IR and XPS analyses [67], and the bending of C-O-C and the length of the C-O bond are indexes for the activation of CO_2.

On the other hand, CeO_2 is a promising adsorbent of CO_2, and the adsorption behavior of CO_2 on CeO_2 has been studied by various methods such as FT-IR, XAS, XPS, DFT-calculations, and so on [66–79]. Particularly, *in-situ* FT-IR analysis is a powerful tool to directly measure the CO_2 adspecies on CeO_2, and four main CO_2 adspecies such as bidentate carbonate, hydrogen carbonate, monodentate carbonate and polydentate carbonate adspecies are proposed to be formed on CeO_2 under pure CO_2 gas flow [59,60]. After the study, the adsorption amount of CO_2 over typical metal oxides such as CeO_2, SiO_2, ZrO_2, and γ-Al_2O_3 was compared by Nomura and co-workers [77], which shows that CeO_2 has a larger CO_2 adsorption amount (~1 μmol m^{-2}, ~130 mmol kg^{-1}) than the other metal oxides and that the hydrogen carbonates are weekly adsorbed on CeO_2 based on FT-IR analysis. These results suggest that CeO_2 is a promising adsorbent of CO_2. If CeO_2 is used for the integrated capture and conversion of CO_2, particularly CO_2 in the air, the CO_2 adsorption amount over CeO_2 from the air and the adsorption state of CO_2 including adsorption/desorption temperatures of CO_2 are important information. Moreover, considering that the air contains water vapor, the effect of water vapor is also of great importance because water vapor can affect the CO_2 adsorption on CeO_2. However, reports on the CO_2 adsorption state over CeO_2 in a low-concentration CO_2 (preferably 0.04 vol%) and the effect of water vapor on the CO_2 adsorption state are very limited, and to our best knowledge, there are two reports by Yoshikawa and co-workers [78,79]. They investigated the effect of water (~3 vol%) on CO_2 adsorption over CeO_2 comparing the CO_2 adsorption amount and CO_2 desorption temperature with/-without water vapor by *in-situ* FT-IR and mass spectroscopies with ~10 vol% CO_2 gas flow [78]. The adsorbed water has little effect on CO_2 adsorption amount on CeO_2 but the desorption of CO_2 adspecies on CeO_2 in the presence of water was easier than that in the absence of water. In the other report [79], they compared the same parameters (CO_2 adsorption amount and CO_2 desorption temperature) with/without water by the same methods with a low CO_2 concentration of CO_2 (0.04 vol%). The CO_2 adsorption amount on the CeO_2 pre-treated by water vapor is a little lower than that without water vapor pretreatment. In addition, the desorption temperature of CO_2 adspecies is higher than that without the water vapor pretreatment. These results are contrary to those of the previous report [78], although the CO_2 concentrations used in these experiments are different (~10 vol% [78] and 0.04 vol% [79]).

As above, the behavior of CO_2 adsorption and desorption on CeO_2 in the presence/absence of water vapor seems to be complicated and remains elusive. In addition, the CO_2 adsorption state on CeO_2 in the presence of water vapor was not discussed in these reports. Therefore, the adsorption behavior and state of CO_2 on CeO_2 under a low concentration of CO_2 with/without water and also the effect of water on CO_2 adsorption on CeO_2 are open to argument. Herein, the adsorption behavior of low concentrations of CO_2 on CeO_2 was investigated by *in-situ* FT-IR, mass spectroscopy, and DFT calculations. In addition, the effect of water vapor on the adsorption of CO_2 on CeO_2 was studied.

2. Experimental

2.1. Preparation of metal oxides

CeO_2 samples were prepared by calcining CeO_2 (CeO_2-HS, DAIICHI KIGENSO KAGAKU KOGYO CO., LTD.) at 873 K for 3 h in air.

2.2. Reagent

5 vol% CO_2/He (standard gas, TAIYO NIPPON SANSO CORP), 0.1 vol% CO_2/He (standard gas, TAIYO NIPPON SANSO CORP), He (G1, TAIYO NIPPON SANSO CORP.) and 5 vol% NH_3/He (standard gas, TAIYO NIPPON SANSO CORP) were used by FT-IR, CO_2 and NH_3-TPD and breakthrough measurements. Water vapor ratio in the mixture gas for FT-IR measurement was adjusted by mixing some introducing gas and He gas passing or not passing through distilled water in some proportion. The water vapor ratio for TPD and breakthrough measurement was adjusted by condensing at a controlled temperature introduced gas passing through distilled water.

2.3. Characterization methods

Specific surface areas of metal oxides were measured with BELSORP MINI X (MicrotracBEL Corporation) by using BET method.

CO_2- and NH_3-temperature-programmed desorption (CO_2- and NH_3-TPD) was carried out by BELCAT II + BELL MASS (MicrotracBEL Corporation) with a cryo cooling system. The samples (~0.1 g) were set in a quartz cell. Before the measurement, the samples were pretreated as follows: the quartz cell including the sample was heated from room temperature to 873 K (pre-treatment temperature) at a rate of 10 K/min under the mixture of He and O_2 (He: 50 mL/min and O_2 10 mL/min) and then held at 873 K for 10 min.

X-ray diffraction (XRD) patterns were recorded using MiniFlex 600 (Rigaku Corporation) with Cu *K*α (40 kV, 15 mA) radiation, and the measurement was conducted with samples in air.

2.4. FT-IR measurement

The sample disks (ϕ 20), which were prepared by using a tablet molder and hydraulic press (20 MPa, 30 s), were located in the *in-situ*

quartz cell with CaF windows and gas lines. The FT-IR spectra were recorded at 4 cm^{-1} resolution in the range from 1000 to 4000 cm^{-1} by FT/IR-6700 (JASCO Corporation) with a deuterated L-alanine triglycine sulphate (DLATGS) detector. CeO_2 was pre-treated at 873 K for 10 min under the mixture of He (30 mL/min) and O_2 (7.5 mL/min) in the cell. The heating rate was 10 K/min. Each FT-IR spectrum was recorded at room temperature under the mixed gas (total flow rate: 30 mL/min). The mixed gas is composed of He (base gas), CO_2 (0, 0.04, 0.1, 1.0, 5.0 vol%), and vapor (0, 0.03, 0.3 vol%). The gases in the measurement system were replaced by He at room temperature under 30 mL/min He for 60 min. The desorption behavior of the CO_2 adspecies on metal oxide was measured by heating the sample cell from room temperature to 873 K under 30 mL/min He. FT-IR spectra are shown as the difference spectra from the spectrum after the pre-treatment unless otherwise noted.

2.5. Quantitative evaluation of adsorbed molecules

Breakthrough measurements were performed by BELCAT II + BEL MASS (MicrotracBEL Corporation) to quantitatively evaluate the equilibrium adsorption amount of CO_2 and water on each sample. A mixed gas containing He (a base gas) and adsorbates (CO_2 or water) was introduced into the sample, and the change in the amount of the adsorbates in the gas passing through the sample was measured as a function of time. For the breakthrough measurements, samples were granulated into 100–150 μm particles, and they were located in the measurement cell (Fig. S1 (I)). Gas was introduced into the measurement cell, and the outlet gas was measured by mass spectroscopy. This experiment was carried out by the following four steps. (1) Pre-treatment: The measurement cell including samples was heated from room temperature to 873 K at the rate of 10 K/min and maintained at 873 K for 10 min under He (50 mL/min) and O_2 (10 mL/min). The cell was cooled down to room temperature under the mixture of He (50 mL/min) and O_2 (10 mL/min). (2) Main step 1 (investigation of mass intensity at saturation): The mixed gas (total flow rate: 30 mL/min) with 0.04, 0.1, 1.0, and 5.0 vol% CO_2/He with or without 0.85 and 1.6 vol% water vapor was introduced to the line 1 at room temperature until saturation of the MASS intensity of CO_2 and water vapor. The gases passing through the line 1 were analyzed by BEL MASS (Fig. S1 (II) connection 1). (3) Main step 2 (breakthrough curve measurement): The mixed gas (total flow rate: 30 mL/min) with 0.04, 0.1, 1.0, and 5.0 vol% CO_2/He with or without 0.85 and 1.6 vol% water vapor was introduced to the measurement cell at room temperature for 30, 120 or 360 min. The gases passing through the sample cell were analyzed by BEL MASS (Fig. S1 (II) connection 2). (4) Desorption: The sample cell was heated from room temperature to 873 K at the rate of 10 K/min and maintained at 873 K for 10 min under He (30 mL/min). And it was cooled down to room temperature under He (30 mL/min). The equilibrium adsorption amount of CO_2 was estimated by the breakthrough curve (Fig. S1). For example, S in Fig. S1 (III) corresponds to the equilibrium adsorption amount of introduced gas. The amounts of stably adsorbed CO_2 were calculated by CO_2-TPD measurements. The humidity of the introducing gas was regulated by changing the temperature of the test tube equipped with a water bubbler at the range of 278–283 K. In the above (1) ~ (3) procedures, the gas lines were heated at 373 K.

In addition, the sequential adsorption of CO_2 and water vapor on the metal oxide samples was conducted with a similar method as shown in the above four steps except for step (4) to observe the behavior of CO_2 adspecies by water vapor introduction. In step (I), pre-treatment was carried out with the same method as shown in the above steps. In step (II), CO_2 was first introduced into the sample. In step (III), water vapor was introduced into the sample with CO_2 adspecies, and the other steps are the same.

3. Results and discussions

3.1. Characterization of metal oxide samples

The CeO_2 sample was characterized by BET surface area, XRD, and CO_2- and NH_3-TPD. The specific surface area of CeO_2 was 91 m^2/g. The results of XRD and CO_2- and NH_3-TPD are shown in Figs. S2 and S3. The base site amount is estimated to be 0.149 mmol g^{-1} (0.0016 mmol m^{-2}) and the acid site amount is done to be 0.169 mmol g^{-1} (0.0019 m^{-2}). CeO_2 has a fluorite structure, and the average particle size is estimated to be 9.9 nm by XRD analysis.

3.2. The adsorption state of CO_2 on CeO_2 at low CO_2 concentration and the dependence of CO_2 concentrations on the CO_2 adsorption on CeO_2

At first, CO_2 adspecies on CeO_2 were measured by FT-IR using mixed gases composed of various concentrations of CO_2 (0.04, 0.1, 1, 5 vol%) and He (base gas). Fig. 1 shows the spectra of CO_2 adspecies on CeO_2 under each CO_2 concentration. The raw spectra of Fig. 1 (I) are shown in Fig. S4 and those of Fig. 1 (III) and (IV) are shown in Fig. S5. Fig. 1 (I) shows the FT-IR spectra at the range of 1000–1800 cm^{-1}, which is the fingerprint region of the CO_2 adspecies. Main signals were observed at 1000–1070, 1217, 1293, 1365, 1399, 1465, 1504, 1572, 1583, and 1599 cm^{-1} when 0.04 vol% and 0.1 vol% CO_2/He were introduced. When 1 vol% and 5 vol% CO_2/He were introduced, the signal at 1413 cm^{-1} was also clearly observed in addition to the above signals. According to the previous report on CO_2 adspecies on CeO_2 by Lavalley and co-workers [70] (Fig. 1 (II) and Table S1), the assignment of these signals are as follows: The signals at 1293 and 1572 cm^{-1} are assignable to bidentate carbonate adspecies on CeO_2. The signals at 1465 cm^{-1} and 1365 cm^{-1} are assignable to polydentate carbonate adspecies on CeO_2. The signals at 1504 cm^{-1} and 1365 cm^{-1} are assigned to monodentate carbonate adspecies on CeO_2, respectively. The signals at 1217, 1399 and 1583 cm^{-1} and those at 1217, 1413 and 1599 cm^{-1} are assignable to two similar hydrogen carbonate adspecies [70]. The former hydrogen carbonate adspecies are observed in all the CO_2 concentrations and strongly adsorbed on CeO_2. The latter hydrogen carbonate adspecies are clearly observed under 1 and 5 vol% CO_2/He and weakly adsorbed on CeO_2.

Fig. 1 (III) and (IV) show the spectra of CO_2 adspecies on CeO_2 at different introduction times in the ranges of 1000–1800 cm^{-1} and 3500–3800 cm^{-1} under 0.1 vol% CO_2/He, respectively. The spectra in the range of 3500–3800 cm^{-1} mainly show the stretching vibrations of hydroxy groups. Main positive signals were observed at 3618 and 3657 cm^{-1} and negative signals were observed at 3669, 3688, and 3716 cm^{-1}, and these signals can be assigned as follows [70]: The positive signal at 3618 cm^{-1} is assignable to ν(OH) of the hydrogen carbonate adspecies on CeO_2 and that at 3657 cm^{-1} is assignable to ν(OH) of bridged hydroxy groups. The negative signal at 3669 cm^{-1} is also assignable to ν(OH) of bridged hydroxyl groups on the CeO_2 surface, that at 3688 cm^{-1} is assignable to ν(OH) of non-dissociated adsorbed water and that at 3716 cm^{-1} is assignable to ν(OH) of on-top hydroxy groups on CeO_2. The positive signal at 3657 cm^{-1} and negative one at 3669 cm^{-1} (Fig. 1 (IV)), which are due to the bridged hydroxy group, are produced by the state change of the bridged hydroxy groups, which can be also seen by the raw spectra of Fig. 1(IV) (Fig. S5 (III)). The signal at 3660 cm^{-1} is assignable to ν(OH) of bridged hydroxy groups and shifted from 3660 cm^{-1} to 3658 cm^{-1} with the time. The signal areas around 3660 cm^{-1} are similar (Fig. S6) all the time. These results suggest that bridged hydroxy groups do not react with CO_2. On the other hand, the intensity of the signal at 3618 cm^{-1}, which is assignable to hydrogen carbonate adspecies, increased and those at 3716 cm^{-1} and 3688 cm^{-1} decreased with time. Considering the signal at 3688 cm^{-1} is attributed to water adspecies, on-top hydroxy groups (observed at 3716 cm^{-1}) react with CO_2 to form the hydrogen carbonate adspecies (Fig. 2). As above, with even low concentrations of CO_2 (0.04 and 0.1 vol% CO_2), similar

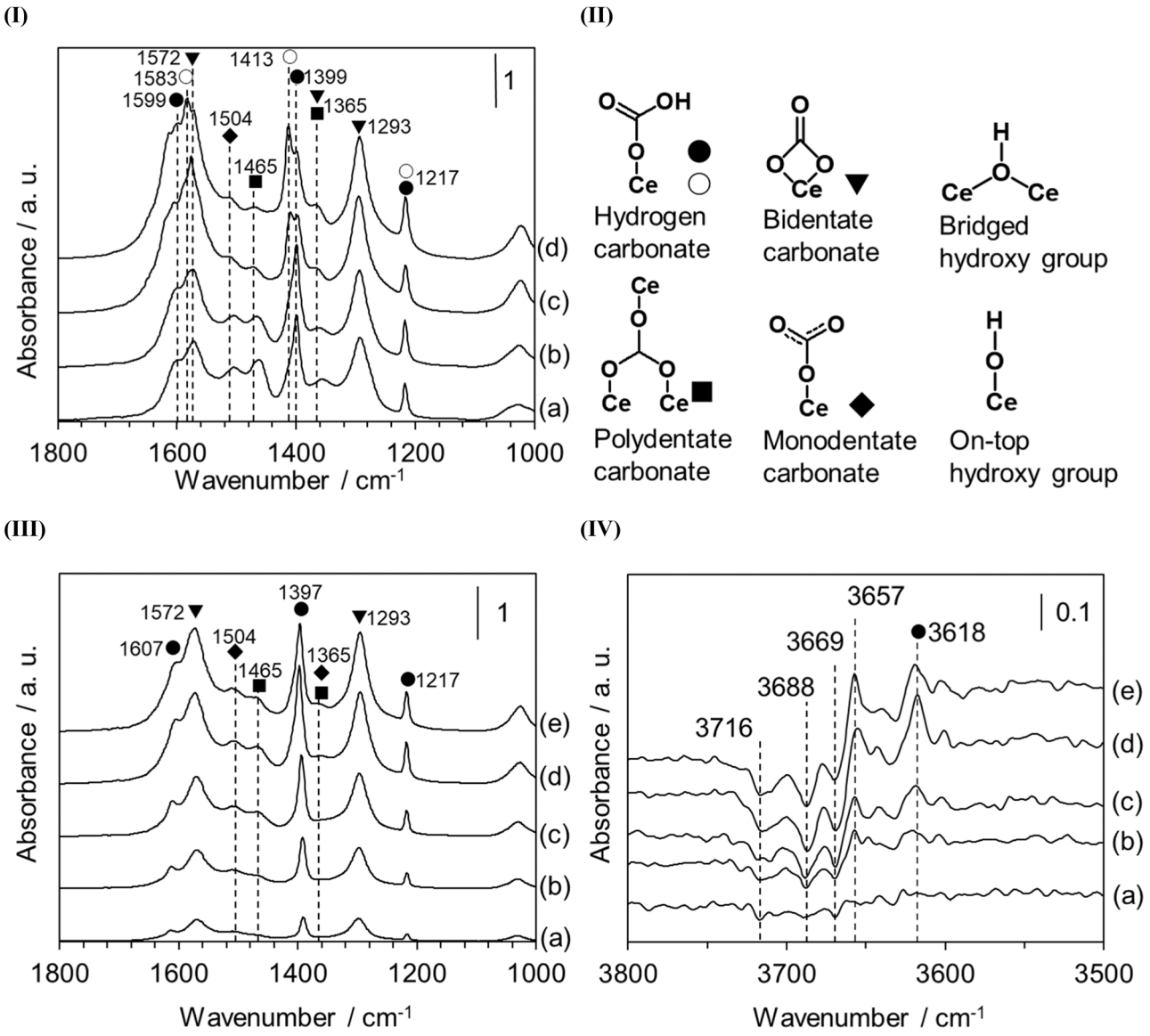

Fig. 1. FT-IR spectra of CO_2 adspecies on CeO_2 at 120 min after introduction of each CO_2 concentration. (I) The spectra at the range of 1000–1800 cm^{-1} after the introduction of 0.04 vol% CO_2 (a), 0.1 vol% CO_2 (b), 1.0 vol% CO_2 (c), and 5.0 vol% CO_2 (d) for 120 min (II) Images of CO_2 adspecies on CeO_2. (III) The spectra at the range of 1000–1800 cm^{-1} after the introduction of 0.1 vol% CO_2 for 10 min (a), 20 min (b), 30 min (c), 60 min (d), and 120 min (e). (IV) The spectra at the range of 3500–3800 cm^{-1} at the conditions of (III). Measurement conditions: CeO_2 60 mg, disk size φ 20, rt, gas flow rate (CO_2 + He) 30 mL/min.

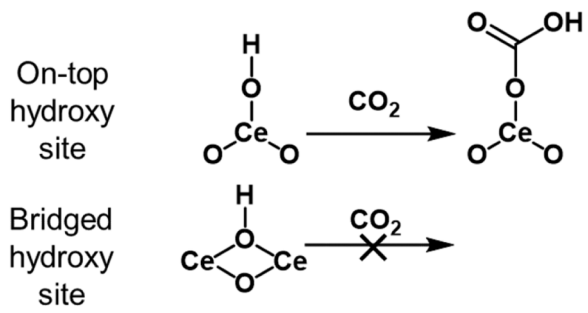

Fig. 2. Image of formation of hydrogen carbonate adspecies from CO_2 and OH adspecies on CeO_2.

CO_2 adspecies to the case of high CO_2 concentrations are formed on CeO_2.

Next, the efficiency of CO_2 adsorption on CeO_2 was evaluated with various concentrations of CO_2. The signal area of 1200–1800 cm^{-1}, which is due to CO_2 adspecies, was plotted as a function of the time (Fig. 3 (I)). The signal area corresponds to the integrated area as shown in Fig. S7 as an example. The signal area increased with time and leveled off at longer times, suggesting that CO_2 adsorption is saturated on CeO_2. The saturation is faster at higher CO_2 concentrations, which is due to the introduction of large CO_2 amounts per time at high CO_2 concentrations. Fig. 3 (II) shows the signal area as a function of the CO_2 introduced amount. In the range of 0–0.01 mmol CO_2 introduced amount, the signal areas at the same CO_2 introduced amount are higher at the concentration of 0.04 vol% and 0.1 vol% than those at the concentrations of 1 vol % and 5 vol%. These results indicated that low concentrations of CO_2 (0.04 or 0.1 vol%) can be effectively adsorbed on the CeO_2 surface.

Moreover, the breakthrough measurement of CO_2 adsorption on CeO_2 was conducted to investigate the efficiency of CO_2 adsorption. The detailed method is shown in the experimental and Fig. S1. The breakthrough curve with 0.04 vol% (400 ppm) CO_2/He is shown in Fig. 4. The CO_2 concentration of the gas passed through the measurement cell including 1.0 g CeO_2, which is calculated from $M/Z = 44$ intensity, is

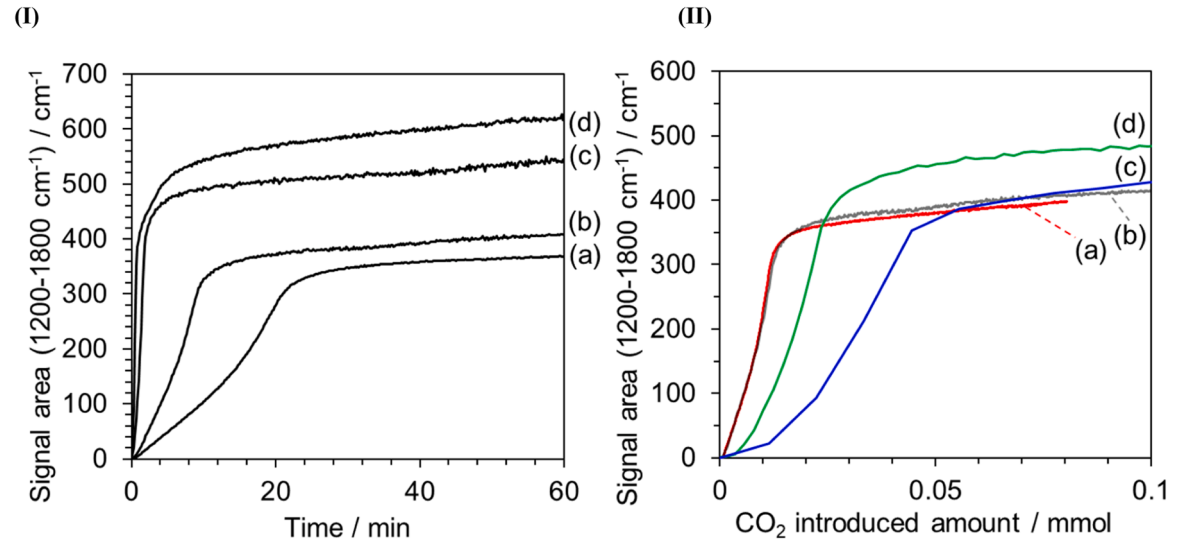

Fig. 3. The change of the signal area (1200–1800 cm^{-1}) of CO_2 adspecies on CeO_2 under different CO_2 concentrations. (I) The signal area (1200–1800 cm^{-1}) as a function of the time. (II) The signal area (1200–1800 cm^{-1}) as a function of introduced CO_2 amount. (a) 0.04 vol% CO_2, (b) 0.1 vol% CO_2, (c) 1 vol% CO_2, and (d) 5 vol% CO_2. Measurement conditions: CeO_2 60 mg, disk size φ 20, rt, gas flow rate (CO_2 + He) 30 mL/min.

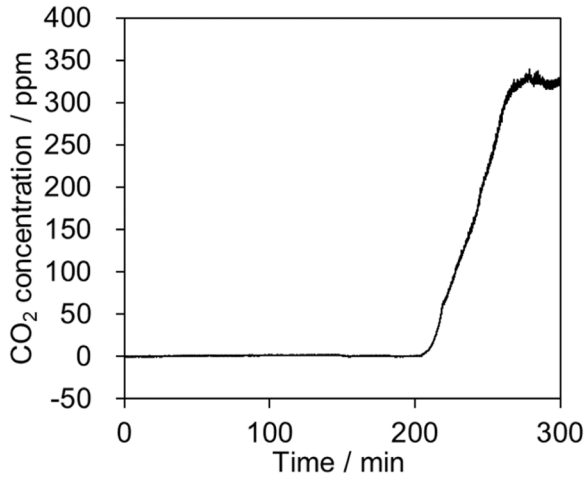

Fig. 4. Breakthrough curve of the introduction of 0.04 vol% CO_2/He into CeO_2. Measurement conditions: CeO_2 1.0 g (100–150 μm grain), adsorption temperature rt, gas flow rate 30 mL/min.

plotted as a function of the time. The signal of $M/Z = 44$ was hardly detected until about 200 min (the detection limitation: CO_2 concentration < 3 ppm), suggesting that 99% and more of CO_2 was adsorbed on CeO_2 even at the low CO_2 concentration of 0.04 vol% (400 ppm). The equilibrium adsorption amount of CO_2 on CeO_2 was calculated by subtracting the detected CO_2 amount by mass spectrometer from the CO_2 introduced amount (Fig. S1(III), red colored area). The equilibrium CO_2 adsorption amount in the case of 0.04 vol% CO_2 is calculated to be 0.13 mmol g^{-1}.

In addition, the CO_2 adsorption amount was also calculated by CO_2-TPD measurement, which is called stable CO_2 adsorption amount in this study. These results are summarized in Table 1 and Table S2 including the signal areas of FT-IR spectra of CO_2 adspecies (Fig. 1 (I)). The equilibrium CO_2 adsorption amount increased with increasing the CO_2 concentration from 0.04 vol% to 1 vol% in the presence and absence of water (Table S2, entries 1–6), which is a similar tendency to the adsorption area of FT-IR measurement (The adsorption of CO_2 in the presence of water vapor is discussed later.). However, the amount of stable CO_2 adsorption amount is almost the same at each CO_2 concentration, indicating that CO_2 is effectively adsorbed on CeO_2 at any CO_2 concentration. From these results, the larger FT-IR signal area under higher CO_2 concentration (Fig. 3) can be explained by the increase in the equilibrium CO_2 adsorption amount.

Table 1
Summary of CO_2 adsorption amount and water adsorption amount.

Entry	Gas		Sample amount /g	TPD measurement (303–873 K)	
	CO_2 concentration /vol%	Water vapor /vol%		Stable CO_2 adsorption amount /mmol g^{-1}	H_2O amount /mmol g^{-1}
1	0.04	~0	0.3	0.12	0.15
2	0.1	~0	0.3	0.12	0.28
3	1	~0	0.3	0.12	0.09
4	0.04	0.85	0.12	0.14	1.00
5	0.04	1.6	0.12	0.14	0.91
6	1	0.85	0.12	0.14	1.06
7	0	0.85	0.12	-	1.02

Fig. S8

As mentioned above, low concentration of CO_2 can be adsorbed on CeO_2 and typical four main CO_2 adspecies can be observed, such as bidentate carbonate, hydrogen carbonate, monodentate carbonate, and polydentate carbonate, which are similar to the CO_2 adspecies on CeO_2 at high CO_2 concentrations. The adsorption efficiency of low concentration of CO_2 on CeO_2 is comparable or high compared with that of high CO_2 concentration. The stable CO_2 adsorption amounts under different CO_2 concentrations are almost the same, while the equilibrium CO_2 adsorption amounts are higher at higher CO_2 concentrations.

3.3. The effect of water vapor on CO_2 adsorption state over CeO_2

The effect of water vapor on the adsorption of CO_2 is important because the actual atmosphere contains at least several hundred ppm of water vapor. At first, the effect of water vapor on the adsorption of CO_2 on CeO_2 was investigated. CO_2 including water vapor (0.03 vol%, 1% humidity) was introduced into CeO_2, and the adspecies were measured by FT-IR (Fig. 5). Up to 30 min (Fig. 5(a)-(c)), the formation of typical CO_2 adspecies such as bidentate carbonate (1297 and 1570 cm^{-1}), polydentate carbonate (1360 cm^{-1} and 1471 cm^{-1}), monodentate carbonate (1360 and 1508 cm^{-1}), and hydrogen carbonate (1217, 1391 and

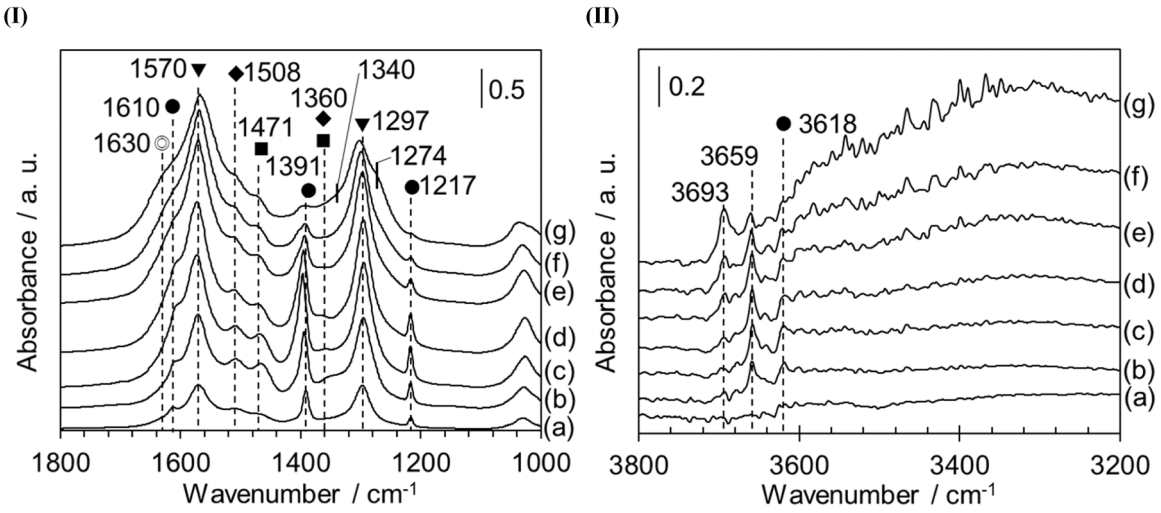

Fig. 5. FT-IR spectra of CO_2 and water adspecies on CeO_2 under 0.04 vol% CO_2/He with water vapor (0.03 vol%). (I) The spectra at 1000–1800 cm^{-1} after 10 min (a), 20 min (b), 30 min (c), 40 min (d) 50 min (e), 60 min (f), and 90 min (g). (II) The spectra at 3200–3800 cm^{-1} at the conditions of (I). Measurement conditions: CeO_2 60 mg, disk size φ 20, rt, gas flow rate (CO_2 + He + water vapor) 30 mL/min.

1610 cm^{-1}) was observed. However, at longer times, the signal due to the hydrogen carbonate adspecies (1217, 1392, and 1610 cm^{-1}) decreased, and new absorption signals (1630, 3693, and around 3300 cm^{-1}), which are due to the adsorbed water molecule on CeO_2, were observed and increased with the time (Fig. 5(d)-(g)). On the other hand, the bidentate carbonate adspecies were not changed, suggesting that the bidentate carbonate adspecies on CeO_2 are stable in the presence of water vapor. New shoulder signals around 1297 cm^{-1} (1274, and 1340 cm^{-1}) were also observed and increased with time. To check the signals due to water adspecies on CeO_2, only water vapor (0.3 vol% in He) was introduced into CeO_2, and the FT-IR spectrum of water adspecies was measured (Fig. S9). Only a broad signal around 1630 cm^{-1} was observed in the range of 1000–1800 cm^{-1}, which is assignable to water adspecies on CeO_2, and there is no signal around 1297 cm^{-1}. These results suggest that the shoulder signals around 1297 cm^{-1} in Fig. 5 is new CO_2 adspecies, which will be formed in the presence of water vapor. It was first confirmed that the hydrogen carbonate adspecies on CeO_2 were converted by water vapor to the new CO_2 adspecies similar to bidentate carbonates based on the time-course of CO_2 adsorption on CeO_2.

Stable CO_2 adsorption amount in the presence of water vapor was measured by CO_2-TPD measurement, and the results are shown in entries 4–6 in Table 1. The stable CO_2 adsorption amount in the presence of water vapor is estimated to be 0.14 mmol g^{-1} at any water concentrations (0.85 and 1.6 vol%), which is about 1.2-fold higher than that in the absence of water vapor (0.12 mmol g^{-1}, entries 1–3). On the other hand, the equilibrium CO_2 adsorption amount, which was determined by the breakthrough measurement, depends on the CO_2 concentrations but was not so influenced by water vapor concentrations (Table S2, entries 1–6). These results indicate that water vapor promotes the adsorption of CO_2 on CeO_2, which tendency is different from that in the previous report [79]. Fig. 6 (I) shows the CO_2-TPD profile in the case of 0.04 vol% CO_2 with and without water vapor. In the absence of water vapor, both weakly adsorbed CO_2 (300–500 K) and strongly adsorbed CO_2 (500–873 K) were clearly observed. In contrast, in the presence of water vapor, weakly adsorbed CO_2 was mainly observed, and strongly adsorbed CO_2 was hardly done. The amount of the weakly adsorbed CO_2 largely increased by the presence of water, leading to the increase of the stable CO_2 adsorption amount (0.12 to 0.14 mmol g^{-1}) as discussed

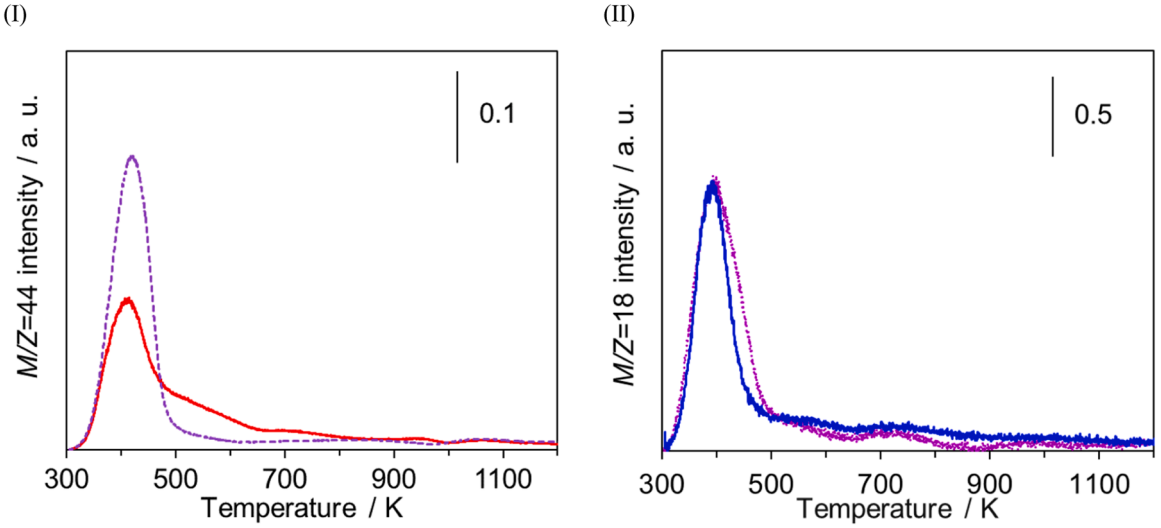

Fig. 6. CO_2- and H_2O-TPD over CeO_2. (I) CO_2-TPD over CeO_2 after the introduction of 0.04 vol% CO_2/He (red line) and 0.04 vol% CO_2/He with water vapor (0.85 vol%) (purple dash line). (II) H_2O-TPD over CeO_2 after the introduction of He with water vapor (blue line) and 0.04 vol% CO_2/He with water vapor (0.85 vol%) (purple dash line). Measurement conditions: CeO_2 300 mg (100–150 μm grain), adsorption temperature rt, gas flow rate (CO_2 + He + water vapor) 30 mL/min.

above. These results suggest that new weakly CO_2 adspecies were formed over CeO_2 in the presence of water. Moreover, H_2O-TPD was also conducted to study the effect of CO_2 on water adsorption on CeO_2 (Fig. 6 (II)). The H_2O-TPD profiles are similar with and without CO_2, and the adsorption amount of water is also similar (Table 1, entries 6 and 7). These results indicate that water is comparatively strongly adsorbed on CeO_2, and that the adsorption is not so inhibited by CO_2 adsorption. Considering the water adsorption amount (1.0 mmol g^{-1}, Table 1) is similar to the surface Ce amount of CeO_2 (~1.1 mmol g^{-1}), the water layer will cover CeO_2. The new weakly adsorbed CO_2 will be adsorbed on the water layer via hydrogen bonding, which is responsible for the increase of CO_2 adsorption amount.

The adsorption strength of CO_2 and water molecules on the CeO_2 surface was investigated by DFT calculations. The CeO_2(111) surface was employed for this investigation since it represents the majority of highly crystallized CeO_2 nanoparticle surfaces due to its lowest surface energy. Four types of adsorption structures have been reported for a CO_2 molecule on the CeO_2(111) surface as described above: monodentate, bidentate, polydentate, and molecular adsorption. The adsorption energies of these structures were calculated to be −0.78, −0.53, −0.66, and −0.27 eV for monodentate, bidentate, polydentate, and molecular adsorption, respectively (see Fig. 7 for each structure). The monodentate structure (Fig. 7(a)) represents the strongest adsorption among these configurations, which is consistent with the previous reports of theoretical calculations [66,76,80,81]. In this structure, both of the two oxygen atoms belonging to CO_2 interact with the surface Ce atoms. The bidentate structure (Fig. 7(b)) involves the interaction between one of the oxygen atoms of CO_2 and the surface Ce atom, and the adsorption energy is weaker than that of the monodentate structure. The polydentate structure (Fig. 7(c)) involves a surface oxygen atom, which is translocated from its original surface position, and this adsorption structure is relatively stable. In the monodentate, bidentate, and polydentate structure, the C−O bond lengths are increased to 1.23 − 1.30 Å, compared to the gas-phase value of 1.18 Å. Also, the O−C−O angles were calculated to be 129, 130, and 120 degrees for monodentate, bidentate, and polydentate structures, respectively, indicating the strong activation of CO_2 molecule. On the other hand, the molecular adsorption (Fig. 7(d)) is relatively weak and involves only the acid-base interaction between one of the oxygen atoms of CO_2 and the surface Ce atom with an adsorption energy of −0.27 eV. Meanwhile, the adsorption energies of a water molecule on the CeO_2(111) surface were found to be −0.68 and −0.69 eV for molecular and dissociative adsorption, respectively (see Fig. S10 for structures). Given that the adsorption energy of the monodentate structure for CO_2 is −0.78 eV, the adsorption of CO_2 and water molecules exhibits a comparable strength.

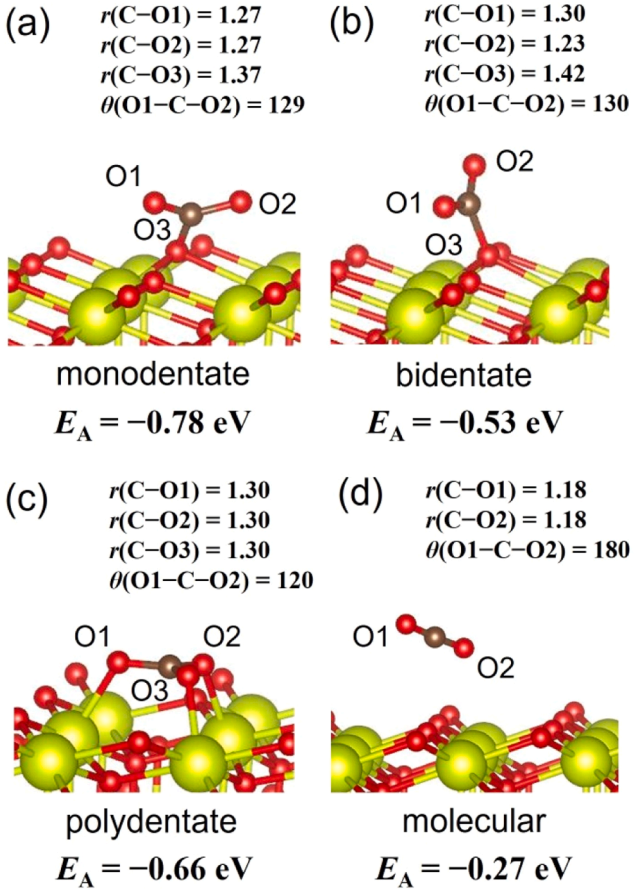

Fig. 7. Adsorption structures of a CO_2 molecule: (a) monodentate, (b) bidentate, (c) polydentate, and (d) molecular adsorption. C−O bond lengths and O−C−O angles are given in Å and degrees, respectively.

The co-adsorption structures of CO_2 and water molecules were next examined. After a thorough investigation of possible structures, the most and second most stable co-adsorption structures are shown in Fig. 8, where the adsorption energies were calculated to be −1.49 and −1.33 eV, respectively. The hydrogen bond is formed between the CO_2 and water molecules, and the CO_2 molecule exhibits a bidentate structure. Considering that the sum of the adsorption energies of the most stable structures of CO_2 (monodentate) and water (dissociative) is −1.47 eV and that of CO_2 (bidentate) and water (dissociative) is −1.22 eV, the co-adsorption of CO_2 and water is feasible. The O−C−O angles and C−O bond lengths are similar to those of CO_2 adspecies without water (Figs. 7 and 8), suggesting that water vapor has little influence on the activation of CO_2. We also found several hydrogen carbonate species after the migration of proton or hydroxide ions from water to the adsorbed CO_2 molecules. The adsorption energies of the most stable structures are shown in Fig. S11, where the adsorption energies of both structures were −1.27 eV. One of the structures involves a hydrogen bond between the oxygen atom of hydrogen carbonate and the surface hydroxy group, and the other one involves the bidentate structure where two oxygen atoms interact with the surface Ce atoms. The adsorption energies of these structures are also comparable to those of co-adsorption structures (Fig. 8), which supports the co-existence of hydrogen carbonate species in experiments. The other possible structures are summarized in Fig. S12. As above, the adsorption energies of water and CO_2 on the CeO_2 surface are comparable, and the co-adsorption of CO_2 and water on CeO_2 is easier than the separate adsorption of CO_2 and water. Therefore, water and CO_2 do not hinder each other's adsorption. These results are also consistent with the results of FT-IR and mass spectroscopies.

Finally, the effect of water vapor on CO_2 adspecies on CeO_2 was studied. Water vapor (0.03 vol%, 1% humidity) was introduced to the

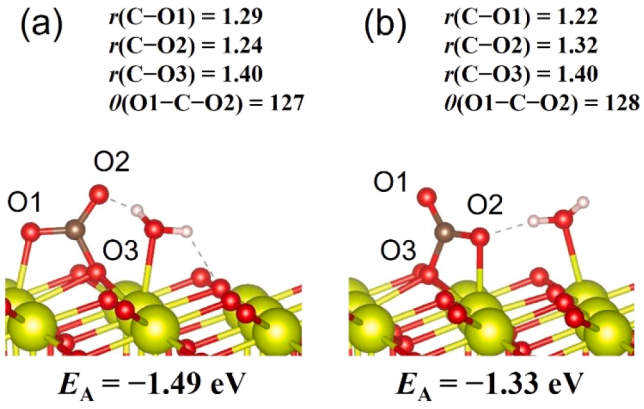

Fig. 8. Co-adsorption structures of CO_2 and water molecule. C−O bond lengths and O-C-O angles are given in Å and degrees.

CO_2-adsorbed CeO_2, and the CO_2 and water adspecies on CeO_2 were measured by FT-IR (Fig. 9). CO_2-adsorbed CeO_2 was prepared beforehand by the introduction of 0.04 vol% CO_2/He into CeO_2 for 120 min. The similar CO_2 adspecies (bidentate carbonate: 1293 and 1570 cm^{-1}, polydentate carbonate: 1362 cm^{-1} and 1465 cm^{-1}, monodentate carbonate: 1360 and 1508 cm^{-1}, hydrogen carbonate: 1217, 1392 and 1611 cm^{-1}) were observed during 30 min after the introduction of water vapor (Fig. 9(I)-(a)-(e)). However, the signals due to the hydrogen carbonate species (1217, 1392, and 1611 cm^{-1}) decreased with time and completely disappeared at 60 min (Fig. 9(I)-(f)). The absorption signals (1630, 3693, and around 3300 cm^{-1}) due to water adspecies on CeO_2 were observed and increased with time, and the shoulder signals around 1293 cm^{-1} (1277, and 1347 cm^{-1}) were observed and increased with time, which tendency is similar to the above case (Fig. 5). In order to check the desorption of CO_2 adspecies on CeO_2 by water vapor, water vapor was introduced into CO_2-adsorbed CeO_2, and the desorbed species were measured by mass analysis. Fig. 10 shows the amount of CO_2 and water in the outlet gas as a function of time. At the initial time, water ($M/Z = 18$) was not detected, however, the amount gradually increased as the time increased. CO_2 ($M/Z = 44$) was not detected at all the measurement time. These results indicate that water was adsorbed on CeO_2 at the initial time and CO_2 adspecies on CeO_2 were not desorbed by water vapor, which result does not contradict the DFT calculations. Considering the result of FT-IR analysis (Fig. 9), the disappearance of the hydrogen carbonate adspecies observed around 1400 cm^{-1} is owing not to the desorption of the adspecies, but to the change of the adsorption state by the interaction with water molecules. The regeneration of the hydrogen carbonate adspecies on CeO_2 was also confirmed by heating the CO_2- and water-adsorbed CeO_2 sample from 298 to 463 K (Fig. S13), which also supports that the state of the hydrogen carbonate adspecies was changed by the interaction with water vapor.

From the above results, the adsorption image of CO_2 and water on CeO_2 in the case of a low concentration of CO_2 is shown in Fig. 11. On-top and bridged OH groups exist on the surface of CeO_2. In the absence of water vapor, bidentate and hydrogen carbonate adspecies are mainly formed by the introduction of CO_2 to CeO_2, and the hydrogen carbonate adspecies are formed by the reaction of CO_2 and an on-top OH group on CeO_2, not a bridged OH group. In the presence of water vapor, both water and CO_2 are adsorbed on CeO_2, and a larger amount of water than CO_2 exists on CeO_2. The bidentate carbonate adspecies are stable in the presence of water vapor, however, the hydrogen carbonate adspecies are not stable and change to a different state by the hydrogen bonding with water. CO_2 is adsorbed on CeO_2 and also on water adspecies of CeO_2 via hydrogen bonding, leading to a larger CO_2 adsorption amount than the case in the absence of water vapor.

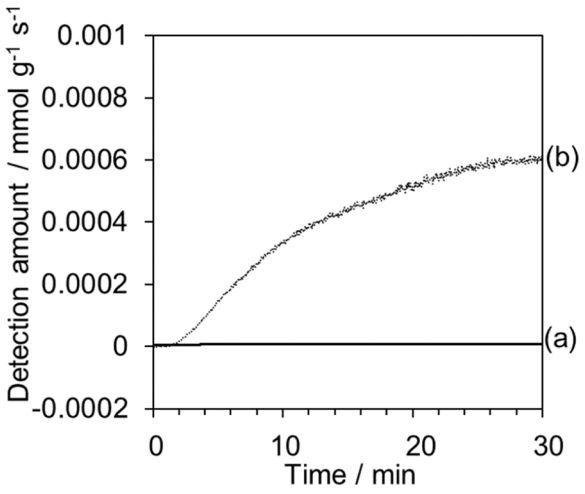

Fig. 10. The time-course of the CO_2 and H_2O amount in the outlet by the introduction of He with water vapor (0.85 vol%) into CO_2-adsorbed CeO_2. (a) CO_2 amount ($M/Z = 44$) and (b) H_2O amount ($M/Z = 18$). Measurement conditions: CeO_2 1.0 g (100–150 μm grain), rt, gas flow rate (He + water vapor) 30 mL/min.

4. Conclusion

The adsorption behavior of low concentration of CO_2 on CeO_2 was investigated by *in situ* FT-IR and mass spectroscopy. The low concentration of CO_2, even atmospheric CO_2 (0.04 vol%), can be easily adsorbed on CeO_2, providing the main four CO_2 adspecies, bidentate carbonate, hydrogen carbonate, monodentate carbonate, and polydentate carbonate adspecies, that are similar to those observed with a high concentration of CO_2. The stable CO_2 adsorption amounts on CeO_2 with different concentrations of CO_2 are similar (~0.12 mmol g^{-1}), although the equilibrium CO_2 adsorption amounts increased with increasing CO_2 concentrations. Moreover, based on the breakthrough measurement, the adsorption efficiency of a low concentration of CO_2 is also high compared with that of a high concentration of CO_2, suggesting a high potential of CeO_2 as the CO_2 absorbent from the air.

The influence of water vapor on the CO_2 adsorption on CeO_2 was also studied by *in situ* FT-IR and mass spectroscopy. Water vapor changed the adsorption state of hydrogen carbonate adspecies via hydrogen bonding, and the stable CO_2 adsorption amount on CeO_2 is higher than that in the absence of water vapor. Based on DFT calculations, the adsorption strength of water and CO_2 are comparable, and CO_2 and water can co-exist because the co-adsorption is stronger via hydrogen bonding than

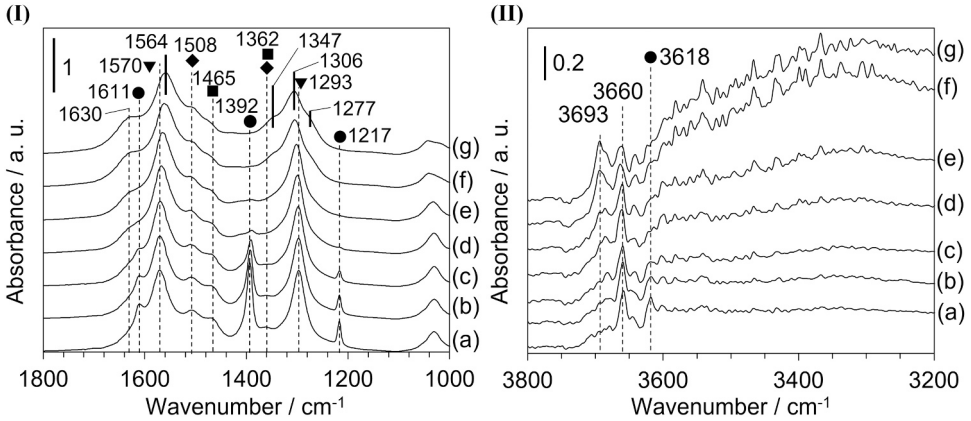

Fig. 9. FT-IR spectra of CO_2 and water adspecies on CeO_2 by the introduction of water vapor (0.03 vol%) into CO_2-adsorbed CeO_2. (I) 1000–1800 cm^{-1} and (II) 3200–3800 cm^{-1}. (a) 0 min, (b) 5 min, (c) 10 min, (d) 20 min, (e) 30 min, (f) 60 min and (g) 90 min. Measurement conditions: CeO_2 60 mg, disk size φ20, rt, gas flow rate (CO_2 + He + water vapor) 30 mL/min.

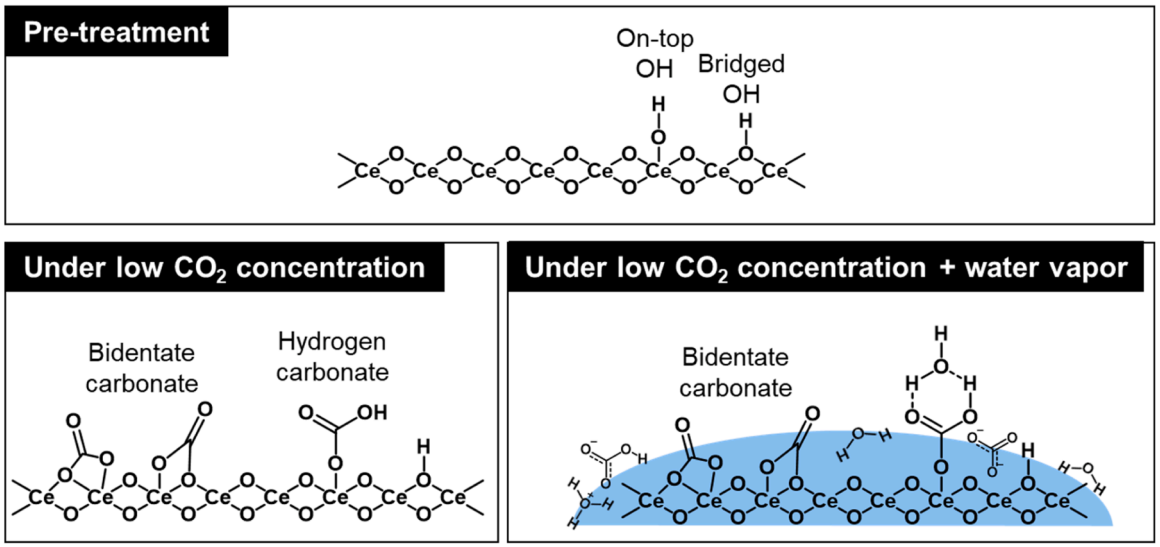

Fig. 11. CO_2 adsorption image with low CO_2 concentration on CeO_2 with and without water vapor.

that of the separative adsorption of CO_2 and water. The adsorbed water on CeO_2 can interact with additional CO_2 via hydrogen bonding, leading to the increase of CO_2 adsorption amount.

CRediT authorship contribution statement

Masato Akatsuka: Writing – review & editing, Formal analysis, Investigation. Akira Nakayama: Formal analysis, Investigation. Masazumi Tamura: Funding acquisition, Conceptualization, Supervision, Formal analysis, Writing – review & editing.

Declaration of Competing Interest

The authors declare that they have no known competing financial interests or personal relationships that could have appeared to influence the work reported in this paper.

Data Availability

Data will be made available on request.

Acknowledgments

This study is based on results obtained from a project commissioned by the New Energy and Industrial Technology Development Organization (NEDO).

Appendix A. Supporting information

Supplementary data associated with this article can be found in the online version at doi:10.1016/j.apcatb.2023.123538.

References

[1] E. Post, R.B. Alley, T.R. Christensen, M. M.-Fauria, B.C. Forbes, M.N. Gooseff, A. Iler, J.T. Kerby, K.L. Laidre, M. Mann, J. Olofsson, J.C. Stroeve, F. Ulmer, R. A. Virginia, M. Wang, The polar regions in a 2 ℃ warmer world, Sci. Adv. 5 (2019) eaaw9883.
[2] X. Yuan, Y. Wang, P. Ji, P. Wu, J. Sheffield, J.A. Otkin, A global transition to flash droughts under climate change, Science 380 (2023) 187–191.
[3] A. Samanta, A. Zhao, G.K.H. Shimizu, P. Sarkar, R. Gupta, Post-combustion CO_2 capture using solid sorbents: a review, Ind. Eng. Chem. Res. 51 (2012) 1438–1464.
[4] J.Y. Lai, L.H. Ngu, S.S. Hashim, A review of CO_2 adsorbents performance for different carbon capture technology processes conditions, *Greenhouse*, Gas. Sci. Tecnol. 11 (2021) 1076–1117.
[5] A. Sodiq, Y. Abdullatif, B. Aissa, A. Ostovar, N. Nassar, M. El-Naas, A. Amhamed, A review on progress made in direct air capture of CO_2, Environ. Technol. Innov. 29 (2023), 102991.
[6] G. Leonzio, P.S. Fennell, N. Shah, A comparative study of different sorbents in the context of direct air capture (DAC): evaluation of key performance indicators and comparisons, Appl. Sci. 12 (2022) 2618.
[7] I. Ghiat, T. Al-Ansari, A review of carbon capture and utilisation as a CO_2 abatement opportunity within the EWF nexus, *J. CO_2 Util.* 45 (2021), 101432.
[8] J.F.D. Tapia, J.-Y. Lee, R.E.H. Ooi, D.C.Y. Foo, R.R. Tan, A review of optimization and decision-making models for the planning of CO_2 capture, utilization and storage (CCUS) systems, *Sustain*, Prod. Consum 13 (2018) 1–15.
[9] E.I. Koytsoumpa, C. Bergins, E. Kakaras, The CO_2 economy: Review of CO_2 capture and reuse technologies, J. Supercrit. Fluids 132 (2018) 3–16.
[10] G. G.-Garcia, M.C. Fernandez, K. Armstrong, S. Woolass, P. Styring, Analytical Review of Life-Cycle Environmental Impacts of Carbon Capture and Utilization Technologies, ChemSusChem 14 (2021) 995–1015.
[11] H.-J. Ho, A. Iizuka, E. Shibata, Carbon Capture and Utilization Technology without Carbon Dioxide Purification and Pressurization: A Review on Its Necessity and Available Technologies, Ind. Eng. Chem. Res. 58 (2019) 8941–8954.
[12] D. Wei, R. Sang, A. Moazezbarabadi, H. Junge, M. Beller, Homogeneous Carbon Capture and Catalytic Hydrogenation: Toward a Chemical Hydrogen Battery System, JACS Au 2 (2022) 1020–1031.
[13] J. Wang, L. Huang, R. Yang, Z. Zhang, J. Wu, Y. Gao, Q. Wang, D. O'Hareb, Z. Zhong, Recent advances in solid sorbents for CO_2 capture and new development trends, Energy Env. Sci. 7 (2014) 3478–3518.
[14] J. Chen, Y. Xu, P. Liao, H. Wang, H. Zhou, Recent Progress in Integrated CO_2 Capture and Conversion Process Using Dual Function Materials: A State-of-the-Art Review, Carbon Capture Sci. Technol. 4 (2022), 100052.
[15] S. Jo, L. Cruz, S. Shah, S. Wasantwisut, A. Phan, K.L.G.-A. Aziz, Perspective on Sorption Enhanced Bifunctional Catalysts to Produce Hydrocarbons, ACS Catal. 12 (2022) 7486–7510.
[16] J. Kothandaraman, R.A. Dagle, V.L. Dagle, S.D. Davidson, E.D. Walter, S.D. Burton, D.W. Hoyt, D.J. Heldebrant, Condensed-phase low temperature heterogeneous hydrogenation of CO_2 to methanol, Catal. Sci. Technol. 8 (2018) 5098–5103.
[17] J. Kothandaraman, D.J. Heldebrant, Towards environmentally benign capture and conversion: heterogeneous metal catalyzed CO_2 hydrogenation in CO_2 capture solvents, Green. Chem. 22 (2020) 828–834.
[18] J. Kothandaraman, J.S. Lopez, Y. Jiang, E.D. Walter, S.D. Burton, R.A. Dagle, D. J. Heldebrant, Integrated Capture and Conversion of CO_2 to Methanol in a Post-Combustion Capture Solvent: Heterogeneous Catalysts for Selective C-N Bond Cleavage, Adv. Energy Mater. 12 (2022) 2202369.
[19] B. Shao, Y. Zhang, Z. Sun, J. Li, Z. Gao, Z. Xie, J. Hu, H. Liu, CO_2 capture and in-situ conversion: recent progresses and perspectives, Green. Chem. Eng. 3 (2022) 189–198.
[20] B. Shao, G. Hu, K.A.M. Alkebsi, G. Ye, X. Lin, W. Du, J. Hu, M. Wang, H. Liu, F. Qian, Heterojunction-redox catalysts of $Fe_xCo_yMg_{10}CaO$ for high-temperature CO_2 capture and in situ conversion in the context of green manufacturing, Energy Environ. Sci. 14 (2021) 2291–2301.
[21] M. Honda, M. Tamura, Y. Nakagawa, K. Tomishige, Catalytic CO_2 conversion to organic carbonates with alcohols in combination with dehydration system, Catal. Sci. Technol. 4 (2014) 2830–2845.
[22] K. Tomishige, Y. Gu, T. Chang, M. Tamura, Y. Nakagawa, Catalytic function of CeO_2 in non-reductive conversion of CO_2 with alcohols, Mater. Today Sustain. 9 (2020).
[23] M. Tamura, K. Shimizu, A. Satsuma, CeO_2-catalyzed Transformations of Nitriles and Amides, Chem. Lett. 41 (2012) 1397–1405.

[24] X. Huang, K. Zhang, B. Peng, G. Wang, M. Muhler, F. Wang, Ceria-Based Materials for Thermocatalytic and Photocatalytic Organic Synthesis, ACS Catal. 11 (2021) 9618–9678.
[25] L. Vivier, D. Duprez, Ceria-Based Solid Catalysts for Organic Chemistry, ChemSusChem 3 (2010) 654–678.
[26] K. Tomishige, M. Tamura, Y. Nakagawa, CO_2 Conversion with Alcohols and Amines into Carbonates, Ureas, and Carbamates over CeO_2 Catalyst in the Presence and Absence of 2-Cyanopyridine, Chem. Rec. 19 (2019) 1354–1379.
[27] M. Tamura, Y. Nakagawa, K. Tomishige, Direct CO_2 Transformation to Aliphatic Polycarbonates, Asian J. Org. Chem. 11 (2022), e202200445.
[28] M. Tamura, M. Honda, Y. Nakagawa, K. Tomishige, Direct conversion of CO_2 with diols, aminoalcohols and diamines to cyclic carbonates, cyclic carbamates and cyclic ureas using heterogeneous catalysts, J. Chem. Technol. Biotechnol. 89 (2014) 19–33.
[29] K. Tomishige, Y. Gu, Y. Nakagawa, M. Tamura, Reaction of CO_2 With Alcohols to Linear-, Cyclic-, and Poly-Carbonates Using CeO_2-Based Catalysts, Front. Energy Res. 8 (2020) 117.
[30] S. Sato, F. Sato, H. Gotoh, Y. Yamada, Selective Dehydration of Alkanediols into Unsaturated Alcohols over Rare Earth Oxide Catalysts, ACS Catal. 3 (2013) 721–734.
[31] M. Honda, S. Kuno, B. Noorjahan, K. K.-i. Fujimoto, Y. Suzuki, Nakagawa, K. Tomishige, Catalytic synthesis of dialkyl carbonate from low pressure CO_2 and alcohols combined with acetonitrile hydration catalyzed by CeO_2, Appl. Catal. A 384 (2010) 165–170.
[32] M. Honda, M. Tamura, Yoshinao Nakagawa, Satoru Sonehara, Kimihito Suzuki, Ken-ichiro Fujimoto, Keiichi Tomishige, Ceria-Catalyzed Conversion of Carbon Dioxide into Dimethyl Carbonate with 2-Cyanopyridine, ChemSusChem 6 (2013) 1341–1344.
[33] A. Bansode, A. Urakawa, Continuous DMC Synthesis from CO_2 and Methanol over a CeO_2 Catalyst in a Fixed Bed Reactor in the Presence of a Dehydrating Agent, ACS Catal. 4 (2014) 3877–3880.
[34] S. Xu, Y. Cao, Z. Liu, Dimethyl carbonate synthesis from CO_2 and methanol over CeO_2-ZrO_2 catalyst, Catal. Commun. 162 (2022), 106397.
[35] M. Tamura, K. Ito, M. Honda, Y. Nakagawa, H. Sugimoto, K. Tomishige, Direct Copolymerization of CO_2 and Diols, Sci. Rep. 6 (2016) 24038.
[36] M. Honda, M. Tamura, K. Nakao, K. Suzuki, Y. Nakagawa, K. Tomishige, Direct Cyclic Carbonate Synthesis from CO_2 and Diol over Carboxylation/Hydration Cascade Catalyst of CeO_2 with 2-Cyanopyridine, ACS Catal. 4 (2014) 1893–1896.
[37] H. Ohno, M. Ikhlayel, M. Tamura, K. Nakao, K. Suzuki, K. Morita, Y. Kato, K. Tomishige, Y. Fukushima, Direct dimethyl carbonate synthesis from CO_2 and methanol catalyzed by CeO_2 and assisted by 2-cyanopyridine: a cradle-to-gate greenhouse gas emission study, Green. Chem. 23 (2021) 457–469.
[38] Y. Gu, K. Matsuda, A. Nakayama, M. Tamura, Y. Nakagawa, K. Tomishige, Direct Synthesis of Alternating Polycarbonates from CO_2 and Diols by Using a Catalyst System of CeO_2 and 2-Furonitrile, ACS Sustain. Chem. Eng. 7 (2019) 6304–6315.
[39] G.G. Giram, V.V. Bokade, S. Darbha, Direct synthesis of diethyl carbonate from ethanol and carbon dioxide over ceria catalysts, N. J. Chem. 42 (2018) 17546–17552.
[40] Y. Gu, M. Tamura, Y. Nakagawa, K. Nakao, K. Suzuki, K. Tomishige, Direct synthesis of polycarbonate diols from atmospheric flow CO_2 and diols without using dehydrating agents, Green. Chem. 23 (2021) 5786–5796.
[41] S.-P. Wang, J.-J. Zhou, S.-Y. Zhao, Y.-J. Zhao, X.-B. Ma, Enhancements of dimethyl carbonate synthesis from methanol and carbon dioxide: The in situ hydrolysis of 2-cyanopyridine and crystal face effect of ceria, Chin. Chem. Lett. 26 (2015) 1096–1100.
[42] M. Honda, S. Sonehara, H. Yasuda, Y. Nakagawa, K. Tomishige, Heterogeneous CeO_2 catalyst for the one-pot synthesis of organic carbamates from amines, CO_2 and alcohols, Green. Chem. 13 (2011) 3406–3413.
[43] M. Honda, A. Suzuki, B. Noorjahan, K. Fujimoto, K. Suzuki, K. Tomishige, Low pressure CO_2 to dimethyl carbonate by the reaction with methanol promoted by acetonitrile hydration, Chem. Commun. (2009) 4596–4598.
[44] M. Honda, M. Tamura, Y. Nakagawa, K. Nakao, K. Suzuki, K. Tomishige, Organic carbonate synthesis from CO_2 and alcohol over CeO_2 with 2-cyanopyridine: Scope and mechanistic studies, J. Catal. 318 (2014) 95–107.
[45] V. Eta, P. M.-Arvela, A.-R. Leino, K. Kordás, T. Salmi, D.Y. Murzin, J.-P. Mikkola, Synthesis of Dimethyl Carbonate from Methanol and Carbon Dioxide: Circumventing Thermodynamic Limitations, Ind. Eng. Chem. Res. 49 (2010) 9609–9617.
[46] M. Honda, S. Kuno, S. Sonehara, K.-i Fujimoto, K. Suzuki, Y. Nakagawa, K. Tomishige, Tandem carboxylation-hydration reaction system from methanol, CO_2 and benzonitrile to dimethyl carbonate and benzamide catalyzed by CeO_2, ChemCatChem 3 (2011) 365–370.
[47] Z.-J. Gong, Y.-R. Li, H.-L. Wu, S.D. Lin, W.-Y. Yu, Direct copolymerization of carbon dioxide and 1,4-butanediol enhanced by ceria nanorod catalyst, Appl. Catal. B 265 (2020), 118524.
[48] Y.-C. Yu, T.-Y. Wang, L.H. Chang, P.-J. Wu, B.-Y. Yu, W.-Y. Yu, J. Taiwan, Inst. Chem. Eng. 116 (2020) 36–42.
[49] M. Tamura, A. Miura, M. Honda, Y. Gu, Y. Nakagawa, K. Tomishige, Direct Catalytic Synthesis of N-Arylcarbamates from CO_2, Anilines and Alcohols, ChemCatChem 10 (2018) 4821–4825.
[50] M. Tamura, M. Honda, K. Noro, Y. Nakagawa, K. Tomishige, Heterogeneous CeO_2-catalyzed selective synthesis of cyclic carbamates from CO_2 and aminoalcohols in acetonitrile solvent, J. Catal. 305 (2013) 191–203.
[51] Y. Gu, A. Miura, M. Tamura, Y. Nakagawa, K. Tomishige, Highly Efficient Synthesis of Alkyl N-Arylcarbamates from CO_2, Anilines, and Branched Alcohols with a Catalyst System of CeO_2 and 2-Cyanopyridine, ACS Sustain. Chem. Eng. 7 (2019) 16795–16802.
[52] M. Tamura, K. Ito, Y. Nakagawa, K. Tomishige, CeO_2-catalyzed direct synthesis of dialkylureas from CO_2 and amines, J. Catal. 343 (2016) 75–85.
[53] M. Tamura, K. Noro, M. Honda, Y. Nakagawa, K. Tomishige, Highly efficient synthesis of cyclic ureas from CO_2 and diamines by a pure CeO_2 catalyst using a 2-propanol solvent, Green. Chem. 15 (2013) 1567–1577.
[54] J. Peng, M. Tamura, M. Yabushita, R. Fujii, Y. Nakagawa, K. Tomishige, CeO_2-Catalyzed Synthesis of 2-Imidazolidinone from Ethylenediamine Carbamate, ACS Omega 6 (2021) 27527–27535.
[55] J. Peng, M. Tamura, M. Yabushita, R. Fujii, Y. Nakagawa, K. Tomishige, CeO_2-catalyzed transformation of various amine carbamates into organic urea derivatives in corresponding amine solvent, Appl. Catal. A 643 (2022), 118747.
[56] R. Fujii, M. Yabushita, D. Asada, M. Tamura, Y. Nakagawa, A. Takahashi, A. Nakayama, K. Tomishige, Continuous Flow Synthesis of 2-Imidazolidinone from Ethylenediamine Carbamate in Ethylenediamine Solvent over the CeO_2 Catalyst: Insights into Catalysis and Deactivation, ACS Catal. 13 (2023) 1562–1573.
[57] M. C.-Cortada, G. Vilé, D. Teschner, J. P.-Ramírez, N. López, Reactivity descriptors for ceria in catalysis, Appl. Catal. B 197 (2016) 299–312.
[58] K. Tomishige, Y. Gu, T. Chang, M. Tamura, Y. Nakagawa, Catalytic function of CeO2 in non-reductive conversion of CO_2 with alcohols, Mater. Today Sustain 9 (2020), 100035.
[59] K. Tomishige, H. Yasuda, Y. Yoshida, M. Nurunnabi, B. Li, K. Kunimori, Catalytic performance and properties of ceria based catalysts for cyclic carbonate synthesis from glycol and carbon dioxide, Green. Chem. 6 (2004) 206–214.
[60] H.J. Lee, S. Park, I.K. Song, J.C. Jung, Direct Synthesis of Dimethyl Carbonate from Methanol and Carbon Dioxide over $Ga_2O_3/Ce_{0.6}Zr_{0.4}O_2$ Catalysts: Effect of Acidity and Basicity of the Catalysts, Catal. Lett. 141 (2011) 531–537.
[61] D. Stoian, F. Medina, A. Urakawa, Improving the Stability of CeO_2 Catalyst by Rare Earth Metal Promotion and Molecular Insights in the Dimethyl Carbonate Synthesis from CO_2 and Methanol with 2-Cyanopyridine, ACS Catal. 8 (2018) 3181–3193.
[62] W. Donphai, O. Phichairatanaphong, R. Fujii, P. Li, T. Chang, M. Yabushita, Y. Nakagawa, K. Tomishige, Synthesis of dimethyl carbonate from CO_2 and methanol over CeO2 catalysts prepared by soft-template precipitation and hydrothermal method, Mater. Today Sustain 24 (2023), 100549.
[63] F. Wang, M. Wei, D.G. Evans, X. Duan, CeO_2-based heterogeneous catalysts toward catalytic conversion of CO_2, J. Mater. Chem. A 4 (2016) 5773–5783.
[64] C.-H. Chung, F.-Y. Tu, T.-A. Chiu, T.-T. Wu, W.-Y. Yu, Critical Roles of Surface Oxygen Vacancy in Heterogeneous Catalysis over Ceria-based Materials: A Selected Review, Chem. Lett. 50 (2021) 856–865.
[65] W.-F. Kuan, C.-H. Chung, M.M. Lin, F.-Y. Tu, Y.-H. Chen, W.-Y. Yu, Activation of carbon dioxide with surface oxygen vacancy of ceria catalyst: An insight from in-situ X-ray absorption near edge structure analysis, Mater. Today Sustain. 23 (2023), 100425.
[66] K.R. Hahn, M. Iannuzzi, A.P. Seitsonen, J. Hutter, Coverage Effect of the CO_2 Adsorption Mechanisms on CeO_2(111) by First Principles Analysis, J. Phys. Chem. C. 117 (2013) 1701–1711.
[67] T. Jin, Y. Zhou, G.J. Mains, J.M. White, J. Phys. Chem. 91 (1987) 5931–5937.
[68] C. Li, Y. Sakata, T. Arai, K. Domen, K. Maruya, T. Onishi, Adsorption of carbon monoxide and carbon dioxide on cerium oxide studied by Fourier-transform infrared spectroscopy. Part 2.—Formation of formate species on partially reduced CeO_2 at room temperature, J. Chem. Soc. Faraday Trans. 1 Phys. Chem. Condens. Phases 85 (1989) 1451–1461.
[69] C. Li, Y. Sakata, T. Arai, K. Domen, K. Maruya, T. Onishi, Carbon monoxide and carbon dioxide adsorption on cerium oxide studied by Fourier-transform infrared spectroscopy. Part 1.—Formation of carbonate species on dehydroxylated CeO_2, at room temperature, J. Chem. Soc. Faraday Trans. 1 Phys. Chem. Condens. Phases 85 (1989) 929–943.
[70] C. Binet, M. Daturi, J.-C. Lavalley, IR study of polycrystalline ceria properties in oxidised and reduced states, Catal. Today 50 (1999) 207–225.
[71] A.A. Azmi, N. Ngadi, M.J. Kamaruddin, Z.Y. Xakaria, L.P. The, N.H.R. Annuar, H. D. Setiabudi, A.A. Jalil, M.A.A. Aziz, Rapid One Pot Synthesis of Mesoporous Ceria Nanoparticles by Sol-gel Method for Enhanced Carbon Dioxide Capture, Chem. Eng. Trans. 72 (2019) 403–408.
[72] Z. Cheng, B.J. Sherman, C.S. Lo, Carbon dioxide activation and dissociation on ceria (110): A density functional theory study, J. Chem. Phys. 138 (2013), 014702.
[73] K. Kanahara, Y. Matsushima, Adsorption and Desorption Properties of CO_2 on CeO_2 Nanoparticles Prepared via Different Synthetic Routes, J. Electrochem. Soc. 166 (2019) B978.
[74] A.H. Ruhaimi, M.A. Ab Aziz, Spherical CeO_2 nanoparticles prepared using an egg-shell membrane as a bio-template for high CO_2 adsorption, Chem. Phys. Lett. 779 (2021), 138842.
[75] C. Slostowski, S. Marre, P. Dagault, O. Babot, T. Toupance, C. Aymonier, CeO_2 nanopowders as solid sorbents for efficient CO_2 capture/release processes, *J. CO_2 Util.* 20 (2017) 52–58.
[76] G.N. Vayssilov, M. Mihaylov, P.St Petkov, K.I. Hadjiivanov, K.M. Neyman, Reassignment of the Vibrational Spectra of Carbonates, Formates, and Related Surface Species on Ceria: A Combined Density Functional and Infrared Spectroscopy Investigation, J. Phys. Chem. C. 115 (2011) 23435–23454.
[77] K. Yoshikawa, H. Sato, M. Kaneeda, J.N. Kondo, Synthesis and analysis of CO_2 adsorbents based on cerium oxide, *J. CO_2 Util.* 8 (2014) 34–38.
[78] K. Yoshikawa, M. Kaneeda, H. Nakamura, Development of Novel CeO_2-based CO_2 adsorbent and analysis on its CO_2 adsorption and desorption mechanism, Energy Procedia 114 (2017) 2481–2487.

[79] K. Yoshikawa, E. Takahashi, T. Miyake, CO_2 Separation from Ambient Air by Novel CeO2-Based Adsorbent, GHGT 14 (2019) 3365769.
[80] N. Baumann, J. Lan, M. Iannuzzi, CO_2 Adsorption on the Pristine and Reduced CeO_2(111) Surface, J. Chem. Phys. 154 (2021), 094702.
[81] X. Lu, W. Wang, S. Wei, C. Guo, Y. Shao, M. Zhang, Z. Deng, H. Zhu, W. Guo, Initial Reduction of CO_2 on Perfect and O-Defective CeO_2(111) Surfaces: Towards CO or COOH? RSC Adv. 5 (2015) 97528–97535.